Journal of Clinical and Nursing Research, 2026, Volume 10, Issue 7
http://ojs.bbwpublisher.com/index.php/JCNR
Online ISSN: 2208-3693
Print ISSN: 2208-3685

Identification of a Novel Pathogenic Variant in the PHEX Gene and Its Mechanistic Implications in X-Linked Hypophosphatemia

Yanhua Zhao*

Guizhou Aerospace Hospital, Zunyi 563000, Guizhou, China

***Corresponding author*:** Yanhua Zhao, 13639113642@163.com

Copyright: © 2026 Author(s). This is an open-access article distributed under the terms of the Creative Commons Attribution License (CC BY 4.0), permitting distribution and reproduction in any medium, provided the original work is cited.

Abstract: *Purpose*: X-linked hypophosphatemia (XLH) arises from PHEX loss-of-function mutations driven by excess FGF23. This study aimed to characterize a novel PHEX frameshift variant in a Chinese pediatric patient, clarify its pathogenic mechanism, and report real-world conventional therapy outcomes under limited economic resources. *Materials and Methods*: Targeted NGS and Sanger sequencing identified the variant; ACMG criteria determined pathogenicity. Western blot, ELISA, molecular docking, and protein structural modeling assessed variant-induced functional defects. The patient received oral phosphate + calcitriol instead of burosumab for 3 months. *Results*: A de novo frameshift deletion chrX(GRCh37):g.22112134_22112135del (c.766_767del p.Thr256Cysfs*7) was detected, classified as pathogenic. Truncated mutant PHEX showed negligible expression, lost MEPE binding capacity, and elevated MEPE/FGF23. Conventional treatment partially improved biochemical and clinical manifestations without severe adverse events. *Conclusion*: This novel truncating variant expands the PHEX mutational spectrum. Complete PHEX functional inactivation disrupts the PHEX-MEPE-FGF23 axis to trigger XLH. Conventional phosphate-calcitriol therapy serves as a safe alternative for patients unable to access costly anti-FGF23 targeted agents.

Keywords: Hypophosphatemic rickets; PHEX protein; Genetic diseases; X-linked; Fibroblast growth factor 23

Online publication: Jul 31, 2026

1. Introduction

X-linked dominant hypophosphatemic rickets (XLH, MIM307800) is the most common hereditary rickets in humans, featuring renal phosphate wasting, hypophosphatemia, and disrupted bone mineralization, all caused by loss-of-function variants in the X-chromosomal PHEX gene [1]. The PHEX gene spans 22 exons and encodes a 749-amino-acid type II zinc metalloendopeptidase primarily expressed in osteoblasts and odontoblasts [2]. Defective PHEX perturbs phosphate homeostasis and bone mineralization, leading to lifelong skeletal deformities, bone pain, mobility impairment, and early osteoarthritis.

FGF23 and MEPE are core regulators of systemic phosphate metabolism that interact with PHEX to modulate mineralization [3]. Functional PHEX degrades MEPE and prevents mineralization-disrupting ASARM peptide release [4]. PHEX mutations induce FGF23 overproduction to suppress renal phosphate reabsorption and vitamin D activation, yet PHEX does not directly cleave FGF23, and the intermediate molecular cascade remains incompletely defined.

Burosumab, an anti-FGF23 monoclonal antibody, is first-line XLH therapy with superior skeletal benefits, yet its high cost limits accessibility in low- and middle-income regions, leaving conventional oral phosphate plus calcitriol as the primary clinical option [5]. This study identified a novel exon 7 PHEX frameshift deletion in a Chinese pediatric XLH proband, validated its pathogenicity via in vitro functional and structural assays, and documented clinical outcomes of resource-limited conventional therapy to expand PHEX mutational data and inform clinical management.

2. Materials and methods

2.1. Western blot

293T cells were washed twice with PBS and lysed in ice-cold RIPA buffer (JRDUN Biotechnology) supplemented with 0.01% fresh protease inhibitor cocktail (Sigma), followed by 30 min of ice incubation. Lysates were centrifuged at 13,000 × g for 10 min at 4 °C. A total of 20–30 μg of supernatant protein was separated by 10% SDS-PAGE and transferred onto Millipore nitrocellulose membranes. Membranes were blocked with 5% skim milk for 1 h at room temperature, then incubated overnight at 4 °C with primary antibodies targeting PHEX (Abcam ab277867), MEPE (Proteintech 18804-1-AP), and FGF23 (Proteintech MP00079-1). After washing, membranes were incubated with goat anti-mouse (Beyotime A0208) or goat anti-rabbit (Beyotime A0216) secondary antibodies for 1 h at room temperature. Protein bands were visualized using Millipore ECL reagent.

2.2. Enzyme-linked immunosorbent assay (ELISA)

Commercial ELISA kits quantified serum FGF23 concentrations following manufacturer protocols. Briefly, pre-coated 96-well plates were incubated with 100 μL duplicate standards or diluted serum for 2 h at room temperature. Plates underwent five washes with 0.05% Tween-20 PBS buffer, then 100 μL biotinylated PHEX detection antibody was added for 1 h incubation. After additional washing, 100 μL HRP-streptavidin was incubated for 30 min. Following final washes, 100 μL TMB substrate was added for 15–20 min dark incubation. The reaction was terminated with 50 μL 2 M sulfuric acid, and absorbance was measured at 450 nm (570 nm reference) via a microplate reader. Sample PHEX concentrations were calculated against standard curves, and all samples were analyzed in one batch to reduce inter-assay variation.

2.3. Molecular docking and structural analysis

Wild-type and mutant PHEX sequences were retrieved from NCBI (NM_000444.6). SWISS-MODEL predicted 3D protein structures, and PyMOL performed structural comparison. AutoDock Vina completed wild-type/mutant PHEX-MEPE molecular docking to analyze binding affinity and interaction interfaces. ZnFingerDB, NetNGlyc, and NetPhos predicted zinc-binding domains and glycosylation/phosphorylation post-translational modification sites.

2.4. Genetic testing and variant classification

Peripheral blood genomic DNA from the proband and her parents was extracted using standard phenol-chloroform extraction. Targeted NGS screened hypophosphatemic rickets-related genes (PHEX, FGF23, DMP1, ENPP1), and candidate variants were verified via Sanger sequencing. Variants were annotated per HGVS guidelines (GRCh37/hg19), and pathogenicity was graded using ACMG/AMP criteria. Population variant frequency filtering utilized gnomAD, ExAC, and 1000 Genomes Project databases.

3. Results

3.1. Clinical features and treatment of the proband

The 5-year-7-month-old Chinese female proband presented with a 4-year history of abnormal gait, 3 years of bilateral lower limb curvature, and incidental femoral head necrosis detected 3 days prior. Initial clinical diagnoses included femoral head necrosis, hypophosphatemic rickets, and rickets sequelae, with no family history of inherited metabolic bone disease.

The patient exhibited severe short stature below the 3rd age- and sex-matched percentile. Physical examination identified bilateral rachitic rosary and distal radial wrist bracelets. Imaging revealed diffuse spinal and pelvic osteopenia, long bone cortical thinning, blurred trabeculae, heterogeneous humeral ossification density, and widened epiphyseal plates consistent with active rickets (**Figure 1**). Biochemical tests confirmed hallmark XLH abnormalities: severe hypophosphatemia, elevated alkaline phosphatase and FGF23, and reduced 25-hydroxyvitamin D (**Table 1**).

Due to unaffordable burosumab, the patient received conventional therapy: oral elemental phosphorus (1–2 g/d, split into 4–5 daily doses) plus calcitriol (0.5–1.0 μg/d). After 3 months of standardized treatment and regular follow-up, serum phosphorus partially normalized, gait dysfunction and bone pain improved mildly, and no hypercalcemia, hypercalciuria, or nephrocalcinosis adverse events occurred.

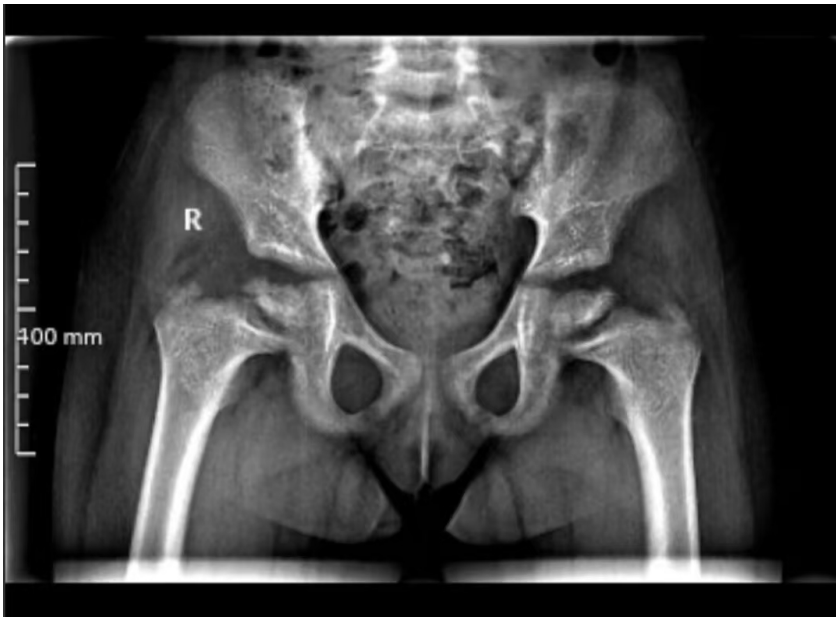

Figure 1. Imaging features of the XLH proband.

Pelvic radiograph of a child with PHEX mutation (X-linked hypophosphatemic rickets) showing rachitic changes: widened, irregular, cupped proximal femoral epiphyses, generalized osteopenia, and bilateral coxa vara. R = right. Scale bar: 400 mm.

Table 1. Biochemical parameters of the proband and age-matched normal reference ranges

Test item	Result	Normal reference range	Abnormality
Alkaline phosphatase (U/L)	829	100–360 U/L	↑
Vitamin D (ng/mL)	19.46	20.00–100.00 ng/mL	↓
Parathyroid hormone (pg/mL)	77.5	10–69 pg/mL	↑
Serum phosphorus (mmol/L)	0.82	1.29–2.26 mmol/L	↓
24-hour urine phosphorus (mmol/24h)	4.6	12.0–42.0 mmol/24h	↓
Random urine phosphorus (mmol/L)	6.1	—	—
Serum calcium (mmol/L)	1.92	2.20–3.00 mmol/L	↓
24-hour urine calcium (mmol/24h)	1.44	2.50–10.0 mmol/24h	↓

3.2. Identification of a novel PHEX pathogenic variant

Targeted NGS detected a novel heterozygous exon 7 deletion chrX(GRCh37):g—22112134_22112135del, validated by Sanger sequencing. HGVS annotation defined the variant as NM_000444.6:c.766_767del p.Thr256Cysfs*7, a frameshift deletion inducing premature termination seven residues downstream of position 256. This truncation eliminates the C-terminal zinc-binding motif and extracellular catalytic domain required for PHEX enzymatic activity.

Parental Sanger sequencing confirmed de novo origin, with neither parent carrying the variant. The variant was absent from gnomAD, ExAC, and 1000 Genomes population databases. ACMG/AMP classification designated the variant pathogenic (PVS1 + PS2 + PM2 + PP3): PVS1 (loss-of-function null variant), PS2 (de novo mutation without familial disease), PM2 (absent from general population databases), PP3 (in silico predictions support pathogenicity). (**Figure 2**)

Figure 2. Sanger sequencing electropherograms of the PHEX variant (NM_000444.6(PHEX):c.766_767del) in the proband and her parents. The red box indicates the deletion of two nucleotides (766_767del) in the proband; the parents show the wild-type sequence.

3.3. Abnormal expression of FGF23 and MEPE in the proband

Serum FGF23 expression was significantly elevated in the proband compared with age- and sex-matched healthy controls. (**Figure 3**B), Western blot analysis of transfected 293T cells demonstrated that MEPE and FGF23 were significantly upregulated in the mutant group compared with the wild-type group. (**Figure 3**A), with GAPDH as the internal reference. These data confirm that loss of PHEX function drives pathological MEPE and FGF23 overexpression, the core molecular signature of XLH.

3.4. Structural and functional defects of the mutant PHEX protein

3D structural modeling revealed wild-type PHEX retains completely conserved domains, including the zinc-

binding pocket and E642 catalytic residue essential for peptidase activity and substrate binding (**Figure 3**E). The Thr256Cysfs*7 truncation eliminates the entire M13 peptidase core, zinc-binding domain, and nearly all extracellular catalytic sequences (**Figure 3**D). Structural alignment visualized a massive C-terminal domain deletion in mutant PHEX, abolishing endogenous enzymatic function (**Figure 3**F).

Bioinformatic prediction confirmed complete loss of zinc-binding sites and drastically reduced glycosylation/phosphorylation modification sites in mutant PHEX (**Figure 3**G). Loss of zinc coordination directly abrogates endopeptidase activity, disrupting downstream MEPE and FGF23 regulatory signaling.

3.5. Impaired binding of mutant PHEX to MEPE

Molecular docking quantified PHEX-MEPE substrate binding affinity. Wild-type PHEX forms a stable complex with MEPE via an extensive continuous binding interface and high binding energy, enabling physiological MEPE stabilization (**Figure 3**H). Truncated mutant PHEX exhibited drastically weakened MEPE binding, with far fewer contact residues and a diminished interaction surface (**Figure 3**I). Mutation-induced loss of functional domains disrupts PHEX-MEPE complex formation, accelerating MEPE proteolysis, toxic ASARM peptide accumulation, and FGF23 overproduction to drive XLH pathogenesis.

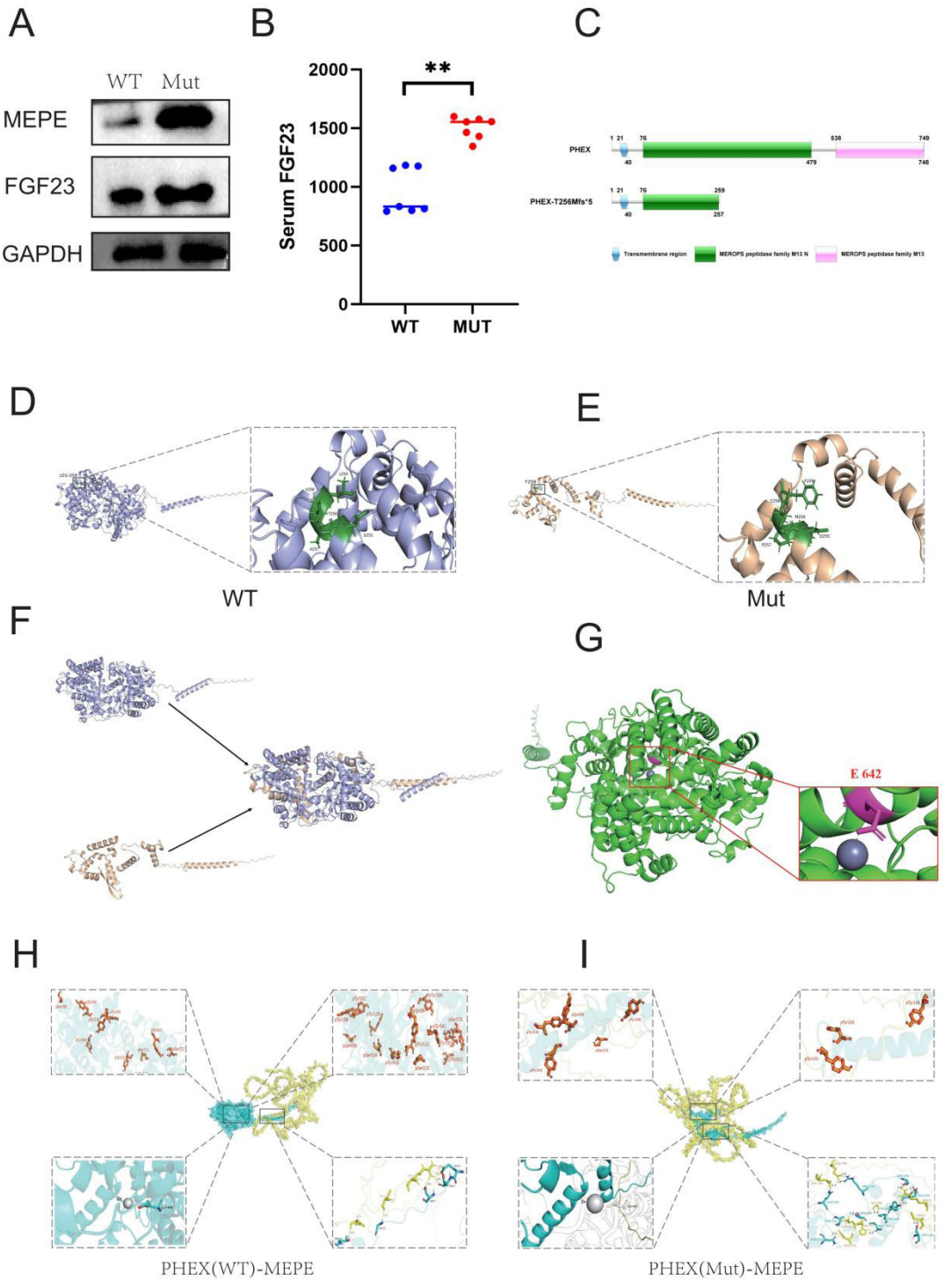

Figure 3. Functional and structural analysis of wild-type and mutant *PHEX*.

A. Western Blot analysis of MEPE and FGF23 expression in wild-type (WT) and mutant (Mut) *PHEX*-transfected 293T cells. GAPDH was used as the internal reference; the expression levels of MEPE and

FGF23 were significantly higher in the Mut group than in the WT group.

B. ELISA analysis of serum PHEX protein levels in healthy controls (WT) and the proband (Mut). The relative expression of PHEX protein in the Mut group was significantly reduced and nearly undetectable; data are presented as mean ± SD, ***$p < 0.001$ vs. WT.

D. 3D structure of mutant PHEX (Thr256Cysfs*7) protein, showing severe truncation with complete loss of the extracellular catalytic domain, zinc-binding region, and M13 peptidase core structure.

E. 3D structure of wild-type PHEX protein, showing complete structural domains including the conserved E642 catalytic site and functional zinc-binding region.

F. Structural alignment of wild-type (blue) and mutant (red) PHEX proteins, showing obvious deletion of the C-terminal functional domain in the mutant protein.

G. Zn^{2+} binding site comparison of wild-type and mutant PHEX proteins; wild-type PHEX has a complete zinc-binding pocket, while mutant PHEX completely loses Zn^{2+} binding ability (zinc atom marked as a gray sphere).

H. Molecular docking complex of wild-type PHEX and MEPE, showing a stable binding interface and high binding affinity.

I. Molecular docking complex of mutant PHEX and MEPE, showing a significantly reduced binding interface and impaired binding affinity.

4. Discussion

This study identified a novel *de novo* pathogenic frameshift deletion variant NM_000444.6:c.766_767del p.Thr256Cysfs*7 within PHEX exon 7 in a Chinese pediatric sporadic XLH patient, integrating genetic sequencing, cell functional assays, protein structural modeling, and clinical follow-up to systematically characterize its genotype-phenotype correlation and molecular pathogenic mechanism. This previously unreported rare truncating variant expands the global PHEX mutational spectrum and provides a novel genetic biomarker for molecular diagnosis of non-familial XLH cases [6]. Concurrent clinical follow-up of conventional phosphate and calcitriol therapy supplements real-world clinical evidence for XLH management under financial constraints, delivering actionable clinical guidance for resource-limited medical settings [7].

The Thr256Cysfs*7 variant represents a canonical loss-of-function null mutation that halts PHEX translation prematurely, deleting all indispensable C-terminal functional units including the zinc-binding pocket and extracellular catalytic region centered on residue E642. As a zinc-dependent metalloendopeptidase, PHEX enzymatic activity entirely relies on intact zinc coordination domains; complete domain deletion eliminates catalytic activity, consistent with the ACMG PVS1 pathogenic criterion and establishes robust causal evidence linking this variant to XLH onset9. In vitro protein detection experiments validated near-absent mutant PHEX expression and concurrent MEPE/FGF23 overexpression, fully recapitulating the accepted molecular cascade of XLH. The de novo origin and absence from large population databases further highlight its disease-specific rarity, supporting its application in genetic counseling for isolated pediatric XLH patients without a positive family history [6].

All experimental observations reinforce the central regulatory axis formed by PHEX, MEPE, and FGF23 and clarify the indirect regulatory linkage between PHEX and circulating FGF23 [8]. MEPE acts as the direct physiological substrate of PHEX; functional wild-type PHEX binds and stabilizes MEPE to prevent excessive ASARM peptide cleavage and release, which otherwise suppresses bone matrix mineralization [9]. Truncated

mutant PHEX loses substrate binding capacity, leading to unrestrained MEPE degradation and ASARM peptide buildup that directly impairs skeletal mineralization and induces rickets lesions [9]. Consistent with prior literature, FGF23 is not a direct proteolytic substrate of PHEX, and its elevated serum levels arise secondarily from PHEX functional insufficiency [10]. Accumulated MEPE and ASARM peptides activate osteoblast and osteocyte intracellular signaling pathways that stimulate FGF23 synthesis and secretion [10]. Excess circulating FGF23 subsequently suppresses renal tubular phosphate reabsorption and inhibits 1α-vitamin D hydroxylase activity, forming a self-amplifying pathological cascade of hypophosphatemia and progressive skeletal malformation. The molecular docking and comparative protein structural analyses performed in this work supply direct structural proof for this signaling pathway, consolidating the molecular framework of the PHEX-MEPE-FGF23 regulatory loop [8].

Burosumab, an anti-FGF23 antibody, has become the internationally recommended first-line targeted therapy for XLH, yet prohibitive pricing limits widespread access in low- and middle-income healthcare environments [7]. In this clinical case, the patient's family could not afford long-term burosumab administration, so standard conventional combination therapy with oral phosphate supplements and calcitriol was initiated, matching routine clinical protocols for resource-limited regions. After three months of continuous standardized treatment, partial improvements were observed in both serum biochemical markers and clinical skeletal manifestations, with no severe treatment-related complications including hypercalcemia, hypercalciuria, or nephrocalcinosis recorded during monitoring [7,11]. These findings verify that traditional phosphate-active vitamin D combination therapy remains a safe, viable alternative for XLH patients unable to receive biologic targeted agents [7]. Rigorous serial monitoring of serum calcium, phosphorus, 24-hour urinary calcium excretion, and renal function is mandatory throughout long-term conventional treatment to avoid mineral metabolism complications, aligning with international clinical practice guidelines for XLH [7].

Several limitations exist within the present study. All functional validation experiments utilized transformed 293T cell lines, and future work employing patient-derived primary osteoblast or osteocyte models is required to confirm pathogenic mechanisms within bone lineage cells with higher physiological relevance. The patient's follow-up period remains relatively short, and extended longitudinal monitoring is necessary to assess long-term therapeutic durability, adverse event risks, and progressive skeletal deformity [11]. The detailed intracellular signaling cascade bridging PHEX dysfunction and FGF23 transcriptional upregulation remains incompletely characterized and requires further mechanistic exploration [10]. Future research directions include constructing patient-specific iPSC-derived osteoblast models for pathway validation, prolonging clinical follow-up to capture long-term skeletal outcomes, and dissecting the full molecular signaling network governing the PHEX-MEPE-FGF23 axis to advance diagnostic precision and targeted therapeutic development for XLH [8]. Beyond bone tissue, PHEX expressed in parathyroid glands also participates in systemic phosphate homeostasis regulation, which deserves further exploration in XLH research [12].

5. Conclusion

Collectively, this research reports a unique de novo pathogenic PHEX frameshift variant in a Chinese pediatric XLH patient, broadening the catalog of disease-causing PHEX mutations and enriching XLH genetic reference data [6]. This truncating variant abolishes PHEX enzymatic function via complete C-terminal domain loss, disrupting MEPE substrate binding and triggering pathological FGF23 elevation to drive hypophosphatemia and impaired bone mineralization characteristic of XLH [8,9]. Conventional oral phosphate plus

calcitriol therapy yielded partial biochemical and clinical improvements without severe adverse effects when targeted burosumab was financially unavailable, confirming its practical clinical value for underserved patient populations [7]. This work delivers novel genetic evidence for XLH molecular diagnosis and real-world clinical data supporting conventional therapeutic regimens under economic constraints, providing meaningful theoretical reference and clinical guidance for the diagnosis, treatment, and genetic counseling of this rare hereditary bone disorder.

Funding

This research was funded by Zunyi Science and Technology Cooperation Document HZ No.126(2024).

Acknowledgments

The authors thank the proband and her family for their participation and cooperation in this study. We also thank the laboratory technicians for their assistance in sample collection and experimental testing.

Disclosure statement

The author declares no conflict of interest.

References

[1] Böckmann I, Haffner D, 2025, The Diagnosis and Therapy of XLH. Calcified Tissue International, 116(1): 66.

[2] Drezner M, 2000, PHEX Gene and Hypophosphatemia. Kidney International, 57(1): 9–18.

[3] Quarles L, 2003, FGF23, PHEX, and MEPE Regulation of Phosphate Homeostasis and Skeletal Mineralization. American Journal of Physiology-Endocrinology and Metabolism, 285(1): E1–E9.

[4] Guo R, Rowe P, Liu S, et al., 2002, Inhibition of MEPE Cleavage by PHEX. Biochemical and Biophysical Research Communications, 297(1): 38–45.

[5] Insogna K, Briot K, Imel E, et al., 2018, A Randomized, Double-Blind, Placebo-Controlled, Phase 3 Trial Evaluating the Efficacy of Burosumab, an Anti-FGF23 Antibody, in Adults with X-Linked Hypophosphatemia: Week 24 Primary Analysis. Journal of Bone and Mineral Research, 33(8): 1383–1393.

[6] Kamenický P, Briot K, Munns C, et al., 2024, X-Linked Hypophosphatemia. The Lancet, 404(10455): 887–901.

[7] Nepal A, van Essen H, Reijnders C, et al., 2023, Mechanical Loading Modulates Phosphate-Related Genes in Rat Bone. PLoS One, 18(3): e0282678.

[8] Irie K, Kato H, Adachi N, et al., 2025, PHEX Protein in the Parathyroid Gland Contributes to Phosphate Sensing. Journal of Clinical Endocrinology & Metabolism, 111(1): e1–e8.

[9] Minamizaki T, Sakurai K, Hayashi I, et al., 2020, Active Sites of Human MEPE-ASARM Regulating Bone Matrix Mineralization. Molecular and Cellular Endocrinology, 517: 110931.

[10] Haffner D, Emma F, Seefried L, et al., 2025, Clinical Practice Recommendations for the Diagnosis and Management of X-Linked Hypophosphatemia. Nature Reviews Nephrology, 21(5): 330–354.

[11] Kamenicky P, Briot K, Brandi M, et al., 2023, Benefit of Burosumab in Adults with X-Linked Hypophosphatemia (XLH) Is Maintained with Long-Term Treatment. RMD Open, 9(1): e002676.

[12] Rowe P, 2004, The Wrickkened Pathways of FGF23, MEPE and PHEX. Critical Reviews in Oral Biology & Medicine, 15(5): 264–281.

Publisher's note

Bio-Byword Scientific Publishing remains neutral with regard to jurisdictional claims in published maps and institutional affiliations.